On the pushover analysis as a method for evaluating the seismic response of RC buildings

P. P. Diotallevi & L. Landi
Department of Civil Engineering DISTART, Bologna University, Italy

Abstract

The purpose of this work was to compare the non-linear pushover and dynamic methods of analysis. Pushover analyses of a RC building were performed considering different load distributions and incremental dynamic analyses were carried out considering a large number of earthquake motions. Then several simplified non-linear procedures based on the pushover analysis were applied in order to assess their capability in the prediction of the seismic demand.
Keywords: non-linear dynamic analysis, pushover analysis, RC buildings, Eurocode 8, simplified non-linear methods.

1 Introduction

In the practical design applications the evaluation of seismic response is usually based on linear elastic structural behaviour. However this approach may be not effective in limiting the damage levels of the buildings. To this purpose more accurate methods of analyses, which can predict the real behaviour under strong seismic actions, are required. The non-linear dynamic analysis is the most rigorous method, but it is still too complex for design use. The non-linear static pushover analysis seems to be a more rational method for estimating the lateral strength and the distribution of inelastic deformations. In the last years several simplified non-linear procedures [1] were developed in order to predict the seismic demand by using the results of pushover analysis. These methods were also implemented in recent guidelines [2, 3] based on the new performance-based engineering concepts.

In the present research the pushover analysis was applied for studying the response of a RC building. Pushover analyses were performed considering different load distributions and incremental dynamic analyses were carried out

considering a large number of earthquake motions. The purpose was to compare the non-linear static and dynamic methods of analysis. Then well-known simplified procedures as the N2 [1] and the capacity spectrum method [4] were used in the evaluation of seismic demand. The aim was to study the differences between the various procedures and to compare them with the dynamic analyses.

2 Analysis method

2.1 Structure under study

The present research was carried out considering a RC frames with six storeys and three spans as structure under study (Fig. 1). The structure was designed according to the new Italian seismic code [5], very similar to the last version of Eurocode 8 [6].

In the design a C25/30 concrete, with a cylinder strength equal to 25 MPa, and a reinforcing steel with a yield strength equal to 430 Mpa were considered. The gravity load amounted to 30 kN/m, and the live load to 12 kN/m. For all beams a rectangular cross-section with a depth of 0.6 m and a width of 0.35 m was assumed. For the columns square cross-sections with variable dimensions from storey to storey were adopted. The dimensions of columns were determined in order to limit the normalized axial force, to give adequate stiffness and to limit the longitudinal reinforcement ratio to values not much larger then 0.01.

The seismic design was performed through a modal analysis considering a response spectrum for medium soil condition and a peak ground acceleration (PGA) equal to 0.35 g. Assuming to develop the design according to the high ductility class, a value of the behaviour factor $q = 5.85$ was assumed. The design moments in columns and the design shear forces in beams and columns were evaluated according to capacity design criteria. In critical regions of beams different tension and compression reinforcement ratios were assumed. The transverse reinforcement in critical regions of beams and columns were defined according to detailing rules for local ductility. In most cases the diameter of stirrups was set equal to 8 mm, and their spacing to 80 mm.

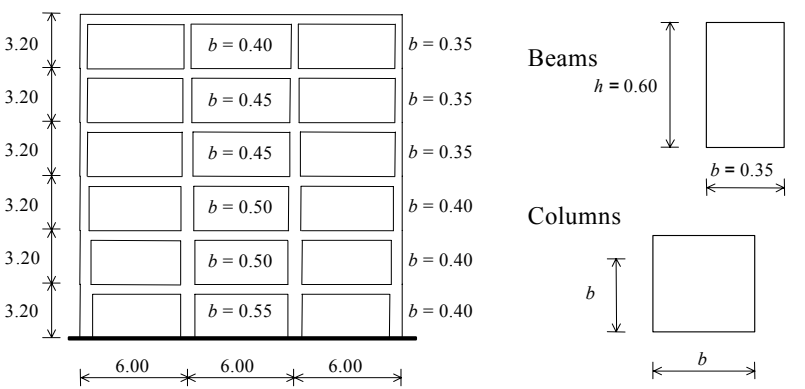

Figure 1: Structure layout.

2.2 Non-linear analysis model

Non-linear static and dynamic analyses of the designed structure were carried out using a computer program based on a non-linear model developed by the authors [7]. The finite element model is characterized by different sub-elements connected in series. They allow to determine the zones, with variable length, where the elastic limit is exceeded, and to account for the principal aspects of the response of RC elements, as the slip of reinforcing bars. The properties of the inelastic zones are derived from those of the control sections, located at the element ends. The behaviour of the control sections is studied with a bilinear moment-curvature relationship for monotonic loading, and with a degrading hysteretic model for cyclic loading. The slope of the elastic branch of the moment-curvature diagram was set equal to the secant stiffness at yield. The analytical model includes also a particular procedure for evaluating the effects of changing axial forces on the loading path of control sections and, as a consequence, on the strength and stiffness of the structural elements.

The deformation capacity of the structural elements was determined in terms of curvature considering the effect of concrete confinement due to stirrups. The concrete law proposed by Scott et al. [8] was adopted. The damage of the structural elements was studied by calculating the ratio of required to available ductility of the control sections. This ratio was calculated at each instant during the loading history, accounting for the actual level of axial load. The ultimate condition of the structure was defined through local and global criteria [9]. The local one identifies the structural collapse with the occurrence of the first flexural or shear collapse of an element. The global one associates the ultimate condition with the exceeding of a given value of the inter-storey drift (3% of the storey high), usually corresponding to the formation of a collapse mechanism.

2.3 Pushover analyses

In the pushover analysis a lateral force distribution representing the inertia forces is applied statically to the structure with increasing intensity until the ultimate condition is exceeded. The global response is represented by the base shear-top displacement curve, called also pushover or capacity curve.

The choice of a proper load shape is a significant aspect because of its influence on the structural response. There is not one only clear criteria to define the load shape, and often one makes reference to literature, guidelines or codes. The Eurocode 8, similar to FEMA 273, requires to use at least two force patterns: one, termed uniform pattern, is based on forces proportional at each storey to the mass, the other, termed modal pattern, is based on forces proportional at each storey to the mass multiplied by the corresponding modal deformation. In general, assuming a load shape related to the displacement shape, the force at a level i can be expressed as:

$$F_i = \frac{m_i \phi_i}{\sum_{j=1}^{N} m_j \phi_j} V_b \tag{1}$$

where m_i and ϕ_i are the mass and the modal deformation of the same level i, V_b is the base shear and N is the total number of storeys. If the deformations ϕ_i are set equal to the deformations of the fundamental mode shape ϕ_{i1}, then the modal patterns is obtained. In the case of flexible or irregular buildings the anticipated effect of the higher modes can be evaluated considering load patterns derived from the combination of different modes [4, 10]. When the elastic limit is exceeded the load shape should be continuously updated during the analysis depending on the level of inelastic deformations. However the adaptive load patterns involve a significant increase of the computational cost.

According to the provisions of EC8 the pushover analyses in the present work were conducted applying both the modal and the uniform load shapes.

2.4 Dynamic analyses

The dynamic analyses were carried out in order to verify the results of the pushover analyses. A set of twenty natural acceleration records, selected within the most frequently used records, was considered. These records, listed elsewhere [11], were obtained during the Imperial Valley (1940), the Irpinia (1980), the Northridge (1994), the Kobe (1995) and other relevant earthquakes. The average response spectrum of the selected records results in good agreement with the code spectrum in the period range of interest [11]. All the acceleration records were scaled to the same PGA value. The dynamic analyses were repeated considering for each record eighteen increasing values of PGA ranging from 0.04 g to 1.2 g. These analyses had the purpose to evaluate the structural response to earthquakes with an increasing intensity.

3 Comparison between dynamic and pushover analyses

Initially the results of the static and dynamic analyses were compared in terms of base shear-top displacement curve. The response of each dynamic analysis was characterized by a point, whose coordinates are the maximum values, during the earthquake, of base shear and top displacement. Through the incremental dynamic analyses it was possible to build for each earthquake record a "dynamic pushover curve" [9]. On the basis of the curves obtained with all records an average and two limit curves, corresponding to the upper and lower envelope, were determined. Figure 2 shows the results of the pushover analyses (POA) for the two load shapes together with the average and the limit curves obtained through the dynamic analyses (NDA).

From Fig. 2 it is clear that the static pushover results are strongly affected by the load shape. Moreover it is evident that the modal pattern provided a better agreement with the average results of the dynamic analyses. However the curve obtained with the uniform pattern is quite close to the upper envelope of the dynamic analyses. Therefore it represents forces and deformations which in certain cases may occur in the structure.

In the elastic range the modal pattern caused a response very close to the average dynamic analyses results, while the uniform pattern determined a larger

stiffness. In the inelastic range the modal pattern gave an underestimation of base shear, while the uniform pattern produced a significant overestimation. However the values of base shear obtained with the modal pattern are closer to the average dynamic analyses results then the values derived with the uniform pattern, and in any case higher then the lower dynamic envelope. The underestimation of the inelastic response with the modal pattern is probably due to the higher modes.

The differences observed between the results obtained with the modal and uniform pattern seems to be in agreement with the observations of other authors [9]. These differences are related with the position of the resultant of lateral load. The resultant of the uniform load distribution is located in a lower position then the resultant of the modal load distribution. To obtain a given displacement the base shear must be larger with the uniform pattern then with the modal pattern. Therefore the uniform load shape tends to provide a conservative estimation of the required strength, particularly of the required shear strength in the elements. On the other hand, the modal load shape tends to provide a conservative prediction of the deformation demand and of the maximum lateral strength.

In Fig. 2 the points corresponding to the first local yield, to the local and to the global collapse condition are marked. The Table 1 shows the values of top displacement, inter-storey drift and base shear associated with the yield and collapse conditions. With the dynamic analyses the average value of base shear associated to the first yield resulted very close to the design value. The average value of PGA that caused the first yield is equal to 0.088 g, larger then the ratio of the design PGA to the design behaviour factor, equal to 0.06 g. With most of the earthquake (fourteen), and also with the pushover analyses, the first yield occurred in the external beam of the third storey.

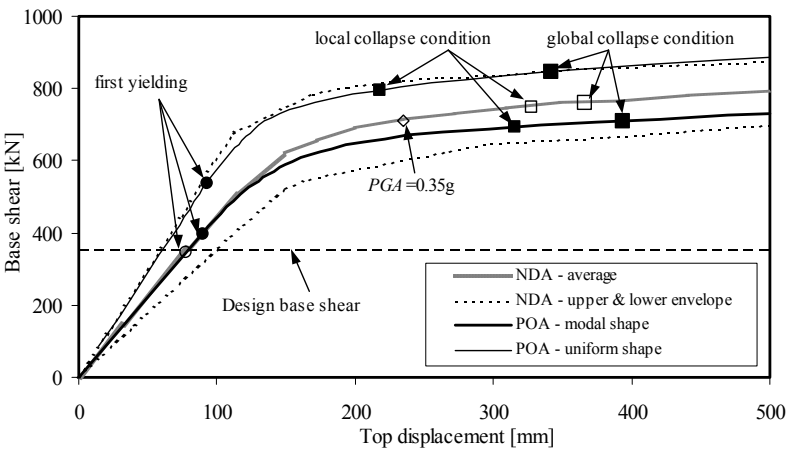

Figure 2: Static pushover and dynamic analysis results.

The points associated with the collapse condition in the average curve of the dynamic analyses and in the pushover curve obtained with the modal pattern

resulted quite close. This shows again that with the modal pattern it is possible to have a good prediction of the seismic response. The average value of PGA that caused the collapse condition is equal to 0.6 g in the case of local collapse, and to 0.65 g in the case of global collapse condition. Both values seemed to be much larger then the design PGA, showing a high safety level of the structure.

Table 1: Response quantities at yielding and collapse conditions.

	First yielding			Local collapse condition			Global collapse condition		
	NDA	POA modal	POA uniform	NDA	POA modal	POA uniform	NDA	POA modal	POA uniform
Top displ. [mm]	77.0	89.5	92.4	327.1	315.5	217.4	365.8	393.1	341.2
Inter-storey drift [mm]	15.9	18.6	21.7	87.7	76.5	59.6	96.0	96.0	96.0
Base shear [kN]	346.1	399.0	538.0	753.4	693.6	795.4	763.5	710.6	846.9

With the uniform pattern the displacement at both local and global collapse condition resulted significantly lower then with the dynamic analyses. Moreover the local collapse occurred much earlier then the global collapse, and the single structural elements collapsed before the formation of a mechanism. This can be seen in Fig. 3, which illustrates the distribution of plastic zones obtained with both load patterns at local collapse. In the same figure the collapsed zone is marked. With most of the earthquake (fifteen), and also with the pushover analyses, the local collapse occurred in a base section of the columns.

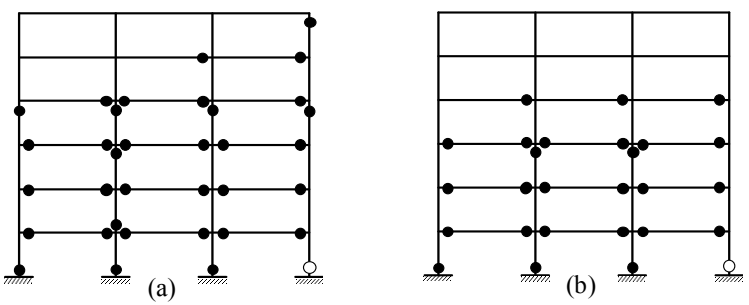

Figure 3: Plastic zones obtained with modal (a) and uniform load shape (b).

The ratio of the base shear at the collapse condition to the base shear at the first yield, called α_u/α_1 in Eurocode 8, corresponds to an overstrength ratio related to the structural redundancy. In the EC8 this ratio, called α_u/α_1, is used in the definition of the behaviour factor, and is set equal to 1.3 for multi-storey and multi-bay frames. Higher values are allowed, but the values assumed cannot be

larger then 1.5, and they have to be confirmed through non-linear analysis. In this research a value of α_u/α_1=1.75 was obtained with the modal pattern, and a value of α_u/α_1=1.5 was obtained with the uniform pattern. Therefore in this case the code provisions seemed to be conservative.

The results of the static and dynamic analyses were compared not only in terms of global response parameters, but also in terms of displacement and ductility demand at the various levels. The comparison was performed considering the results of pushover analyses in correspondence with a top displacement equal to the average value obtained from the dynamic analyses with the earthquake records scaled to the design PGA.

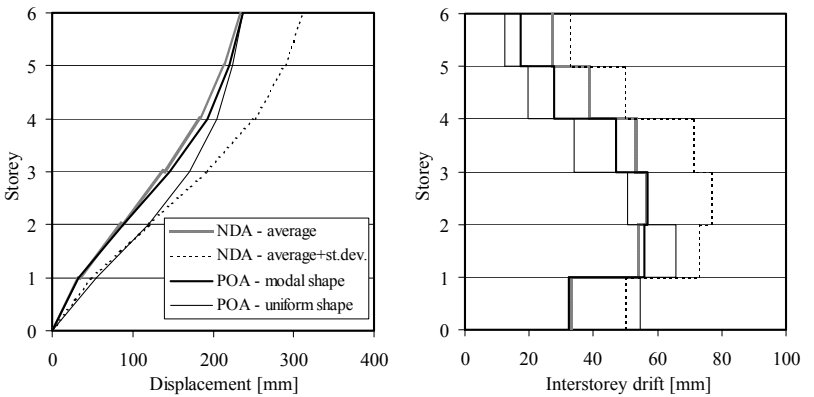

Figure 4: Distribution of displacement and inter-storey drift.

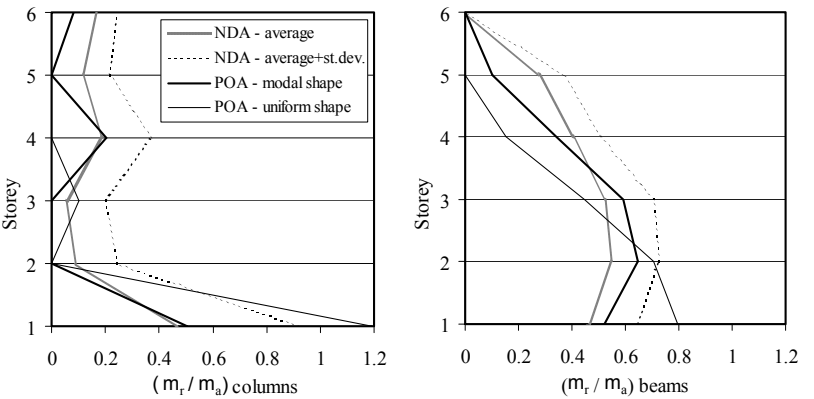

Figure 5: Distribution of damage in beams and columns.

Figure 4 shows the diagrams of displacement and inter-storey drift along the height of the building, while the Figure 5 displays the diagram of damage in beams and columns. The displacement diagram obtained with the modal shape

and with the dynamic analyses resulted very similar. The modal shape caused values slightly larger then the dynamic analyses at the fourth and fifth floors. The pushover analysis with uniform load shape produced a different displacement diagram, with much larger values then the other methods of analysis at the first three floors. The inter-storey drift diagram reflects what observed about the different position of the resultant of the two load distributions. Moving from the modal to the uniform load pattern the drop of the position of the resultant caused a significant increment of inter-storey drift at the first two storeys, and a reduction at the higher storeys. On the contrary the modal shape provided values very similar to those of the dynamic analyses at the first three storeys. Moreover the modal shape was capable to predict with enough accuracy the maximum value, and the storey where this value was attained.

In Figure 5 the maximum of the values calculated in beams and columns at each storey of the ratio of required to available ductility is reported. As observed about the inter-storey drift diagram, the uniform shape caused larger values at the first two storeys and lower values at the higher storeys then the other methods of analysis. The diagram of damage in columns obtained with the modal pattern seems to be similar to that of the dynamic analyses. As a consequence of capacity design criteria the damage of columns was concentrated at the base, while the damage of beams was more distributed along the height.

4 Determination of the seismic demand through simplified methods

4.1 Capacity spectrum

Within the simplified procedures the seismic demand is usually evaluated by using the response spectra or the time-history analysis with reference to a Single-Degree-of-Freedom (SDOF) system. Therefore the structure under study needs to be transformed into an equivalent SDOF system. The following description refers to the procedure used by Fajfar [1], which has the peculiarity of adopting a displacement shape related to the load shape through the equation (1). The force-displacement curve of the SDOF system is obtained by means of the equations:

$$D_t = D^* \Gamma \tag{2}$$

$$V_b = F^* \Gamma \tag{3}$$

where D^* and F^* are the force and displacement of the SDOF system, and D_t is the top displacement of the MDOF structure. The constant Γ is the modal participation factor of the assumed displacement shape, and is defined as:

$$\Gamma = \frac{\sum_{i=1}^{N} m_i \phi_i}{\sum_{i=1}^{N} m_i \phi_i^2} \tag{4}$$

where m_i is the storey mass, and ϕ_i is storey deformation normalized in order to have unity value at the top. The value in the numerator is the equivalent mass m^*:

$$m^* = \sum_{i=1}^{N} m_i \phi_i \tag{5}$$

The initial stiffness of the equivalent SDOF system is equal to that of the MDOF system since forces and displacement are transformed in the same way. The use of response spectra for the seismic analysis of the SDOF system requires an additional step, i.e. the determination of a bilinear idealization for the capacity curve. This is a significant aspect since it provides the dynamic properties of the equivalent SDOF system. When the bilinear diagram is known the fundamental period T^* of the equivalent SDOF system can be calculated. The capacity spectrum is finally obtained by representing the capacity curve in the ADRS (Acceleration-Displacement Response Spectrum) format. The spectral acceleration is determined dividing the forces F^* by the equivalent mass m^*.

4.2 Methods for the determination of the seismic demand

As it was previously seen the seismic demand may be determined by using the response spectra. Since in general the seismic response is non-linear, the use of inelastic spectra is necessary. Several simplified methods are based on the capacity spectrum method, originally developed by Freeman [4]. This method uses highly damped elastic spectra to account for the energy dissipation due to the hysteretic behaviour of the structure. As an alternative other authors [13] proposed to use the constant ductility spectra, which can be obtained by applying to the elastic spectrum a reduction factor R_μ related to ductility.

4.2.1 N2 method

The N2 method, developed by Fajfar and Gasperic [12] with the purpose to estimate the seismic damage of RC structure, was then formulated in the ADRS format as modified capacity spectrum method [13]. The bilinear idealization of the capacity curve is characterized by a zero post-yield stiffness since the influence of moderate strain hardening is included in the demand spectrum. The secant stiffness at a force equal to 60 % of the yield strength is adopted as elastic stiffness. The elastic limit is determined by imposing that the areas under the original and idealized curve are equal.

The acceleration S_a and the displacement S_d in the inelastic spectrum are determined from the corresponding quantities S_{ae} and S_{de} in the elastic spectrum through the following relations:

$$S_a = \frac{S_{ae}}{R_\mu} \tag{6}$$

$$S_d = \frac{\mu}{R_\mu} S_{de} = \frac{\mu}{R_\mu} \frac{T^2}{4\pi^2} S_{ae} \tag{7}$$

being μ the ductility and R_μ the reduction factor of the elastic spectrum. The latter is calculated using the formulae proposed by Vidic et al. [14], based on the equal displacement rule in the range of medium-long periods:

$$R_\mu = (\mu - 1)\frac{T}{T_0} + 1, \quad T \le T_0 \tag{8}$$

$$R_\mu = \mu, \quad T \ge T_0 \tag{9}$$

$$T_0 = 0.65\mu^{0.3} T_c \le T_c \tag{10}$$

where T_c is the characteristic period of the ground motion.

The procedure for determining the seismic demand is made by the following steps. Initially the acceleration S_{ae} and the displacement S_{de} in the elastic spectrum are calculated as functions of the period T^* of the equivalent SDOF system. In the ADRS format the intersection of the elastic spectrum and of the radial line corresponding to T^* is determined. If T^* is larger then T_0, the inelastic displacement demand of the SDOF system is equal to the elastic displacement S_{de}. If T^* is lower then T_0, the reduction factor R_μ has to be calculated. This factor can be determined as the ratio between S_{ae} and the yield acceleration S_{ay} of the SDOF system. Knowing R_μ it is possible to obtain the required ductility by rearranging the equation (8). Since also T_0 depends on the ductility, the use of equation (8) may require iterations.

A simplified version of the N2 method was implemented in the Final Draft of Eurocode 8 [6]. Considering $T_0 = T_c$ a simplified expression of the reduction factor is obtained. Also the elastic-plastic idealization of the capacity curve is determined with another method. The yield strength is set equal to the peak force of the capacity curve. The elastic stiffness is determined by equating the areas under the original and idealized curve in a range delimited by the displacement at the formation of plastic mechanism.

4.2.2 Capacity spectrum method

The capacity spectrum method is based on the comparison between the capacity spectrum and the highly damped elastic spectra in the ADRS format. Since the equivalent viscous damping depends on the displacement demand, the quantities which govern the problem are interrelated, and iterations are needed.

In the guidelines ATC-40 [2] three procedures, called A, B and C, were developed for the application of the capacity spectrum method. The procedure A represents the direct application of the method, while the procedures B and C introduce some approximations. Denoting with a and d the acceleration and displacement in the ADRS format, the first step is the selection of a point a_{pi}, d_{pi} of the capacity spectrum as trial position of the performance point. As initial point the intersection of the radial line corresponding to the elastic period and the 5% damped response spectrum can be assumed. The bilinear representation of the capacity spectrum is characterized by an elastic stiffness equal to the initial stiffness, and by a post-elastic branch passing through the point a_{pi}, d_{pi}. The

elastic limit a_y, d_y is determined by imposing that the areas under the original and idealized curve are equal. The equivalent damping is calculated as follows:

$$\beta_{eq} = 5 + \kappa\beta_0 = 5 + \kappa 63.7 \frac{a_y d_{pi} - a_{pi} d_y}{a_{pi} d_{pi}} \tag{11}$$

where β_0 is the viscous damping equivalent to the energy dissipated in a loading cycle by a bilinear system, and κ is a reduction factor taking account for the degradation of cyclic response. This factor is defined in a table as a function of β_0 and of the behaviour type, which is classified in three categories according to the lateral resisting system and to the shaking duration.

The elastic spectrum related to the damping β_{eq} is obtained by applying the reduction factors SR_A and SR_V to the ordinates of the 5% damped response spectrum. SR_A is used in the constant acceleration zone of the spectrum, SR_V in the constant velocity zone. They are calculated as functions of the damping β_{eq}. If the highly damped response spectrum does intersect the capacity spectrum in a point within acceptable tolerance of d_{pi}, then the trial point is the performance point. Otherwise a new point a_{pi}, d_{pi} have to be selected and the procedure is repeated. The procedure B assumes that the bilinear idealization remains constant during the iterations, while the procedure C is characterized by a graphical method which does not require iterations.

4.2.3 Displacement coefficient method

This method, implemented in the guidelines FEMA 273 [3], provides directly the estimation of the maximum top displacement δ_{TOP} without requiring the conversion in spectral coordinates and the execution of iterations. The bilinear idealization of the capacity curve is determined by fixing the post-elastic branch and considering as elastic stiffness the secant stiffness at a force equal to 60 % of the yield strength. The displacement demand is calculated on the basis of the inelastic displacement spectra, which are obtained from the elastic spectra through different modification factors:

$$\delta_{TOP} = C_0 C_1 C_2 C_3 S_a \frac{T_e^2}{4\pi^2} \tag{12}$$

being T_e the fundamental period of the structure calculated considering the elastic stiffness of the bilinear diagram, and S_a the elastic spectral acceleration. C_0 relates the spectral to the top displacement, C_1 relates the inelastic to the elastic spectral displacement, C_2 represents the effect of hysteresis shape and C_3 accounts for the second-order effects.

4.3 Applications

The procedures above described were applied to the structure under study. In the use of all the simplified methods the same elastic response spectrum, corresponding to the design one, was adopted. The simplified methods were applied considering the capacity curve obtained with the modal load distribution. The modal participation factor of the assumed deformed shape resulted $\Gamma = 1.32$.

The top displacement and the base shear at the collapse condition are D_{tu} = 315 mm and V_{bu} = 693 kN for the structure, and D^*_u = 238 mm and F^*_u = 525 kN for the equivalent SDOF system.

In the application of the N2 method the secant stiffness at the 60 % of the yield strength seemed to be almost equal to the initial stiffness. This was due to the adoption of the secant stiffness at yield as elastic stiffness for the structural elements. The fundamental period of the equivalent SDOF system was T^* = 1.55 sec. From the ratio between S_{ae} and S_{ay} the reduction factor, equal to R_μ = 1.89, was calculated. Since T^* was larger then T_c the displacement demand of the SDOF system was equal to the elastic spectral displacement S_{de} = 211 mm (Fig. 6), and the top displacement of the structure resulted D_t = 278 mm.

By using the procedure of EC8 an elastic-plastic diagram with a lower elastic stiffness was obtained. In this case the fundamental period resulted T^* = 1.65 sec. Since T^* was larger then T_c the simplified inelastic spectra resulted equal to those determined with the Vidic formulae. Therefore in the present application the only difference between the N2 method and the EC8 was the value of T^*. With this value the displacement demand of the SDOF system was equal to 225 mm (Fig. 6), slightly larger then the value obtained with the N2 method, and the top displacement resulted D_t = 297 mm. The procedure of EC8 usually tends to provide an overestimation of the displacement demand. This is due to the method for determining the elastic-plastic idealization. When the displacement demand is much lower then that at the plastic mechanism, it is reasonable to adopt larger values of elastic stiffness [1]. Moreover when the initial portion of the capacity curve is almost linear up to the elastic limit, as in the case under study, it is reasonable to consider an elastic stiffness close to the initial one.

The capacity spectrum method was applied according to the procedure A (Fig. 7) and B of the ATC-40. The procedure A provided at convergence a displacement demand d_{pi} = 179 mm. The equivalent damping calculated with the relation (11) resulted equal to 18.4 %. The procedure B provided a displacement demand d_{pi} = 176 mm, very close to the value obtained with the procedure A. Generally the procedure B tends to give similar values to the procedure A if the performance point is not much away from the point initially used to determine the bilinear diagram. The top displacement of the structure with the procedures A and B resulted equal to 236 and 233 mm.

In the case of the displacement coefficient method the bilinear idealization of the capacity curve was characterized by the same elastic stiffness as in the N2 method. Therefore the elastic spectral acceleration was calculated as a function of the period T^* = 1.55 sec. The factor C_0 was set equal to Γ, i.e. to 1.32, the factor C_2 was set equal to 1.1, according to the tables provided by the FEMA 273, while for the factors C_1 and C_2 a unity value was considered. With these values of the modification factors the relation (12) gave a top displacement δ_{TOP} = 306 mm. If a unity value was considered also for C_2, the same top displacement of the N2 method was provided.

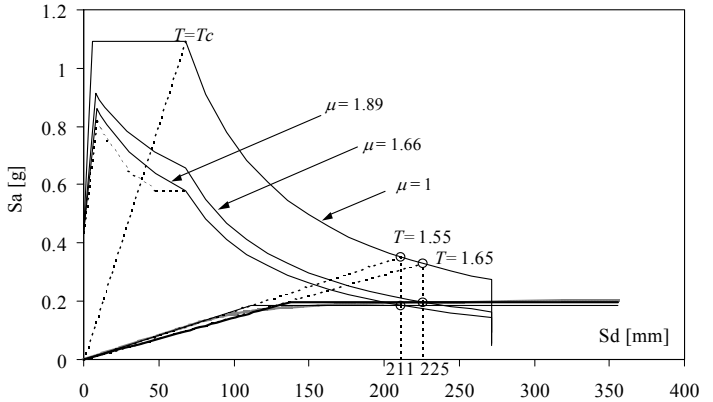

Figure 6: Seismic demand with N2 and EC8 methods.

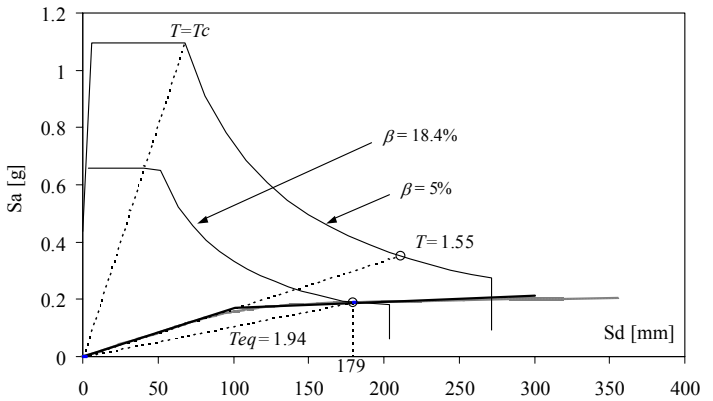

Figure 7: Seismic demand with ATC-40 procedure A.

Table 2 shows all the values obtained with the different simplified methods together with the average dynamic analyses results. The procedures of ATC-40 provided values very close to the average dynamic analyses results, while the other methods gave more conservative values. In any case a good agreement between the simplified methods and the dynamic analyses was found. The values obtained with the simplified methods resulted all included between the average dynamic analyses results and the sum of the average value with the standard deviation. With reference to the structural behaviour it is possible to observe that the displacement values obtained with the simplified methods are lower then the displacement at the local collapse condition, showing that the structure did satisfy the seismic safety requirement at the ultimate limit state.

Table 2: Comparison between the simplified methods.

ATC-40a	ATC-40b	FEMA	N2	EC8	NDA (average)	NDA (average + st. dev.)
236.8	233.4	306.4	278.6	297.6	234.7	311.7

5 Conclusions

Pushover and a large number of dynamic analyses were carried out on a RC frame building, then several simplified methods were applied in order to predict the seismic demand. It is necessary to state that the conclusions are applicable to the considered structural configuration. The study should be extended in order to comprehend other structural configurations.

The pushover curves resulted strongly affected by the assumed lateral load distribution. The modal shape provided the best agreement with the average results of the dynamic analyses. It also provided a conservative estimation of the lateral strength and a good prediction of the deformation capacity. Moreover the damage distribution obtained with the modal shape was very similar to that obtained through dynamic analyses. The uniform load distribution gave results close to the upper envelope of the dynamic analyses results. This distribution should be considered in addition to the modal shape unless more sophisticated pushover methods are used.

All the used simplified methods provided a good agreement with the dynamic analyses results. The best agreement was obtained with the procedures of the ATC-40, while more conservative results were obtained with the other methods. The relations which define the demand spectra had a great influence, but also the method to determine the bilinear idealization of the capacity curve did significantly affect the results.

References

[1] Fajfar, P., Structural analysis in earthquake engineering – a breakthrough of simplified non-linear methods, Proc. of the 12th European Conf. on Earthquake Engineering, London, 2002.

[2] ATC, Seismic evaluation and retrofit of concrete buildings, Vol. 1, ATC-40, Applied Technology Council, Redwood City, 1996.

[3] BSSC, NEHRP Guidelines for the seismic rehabilitation of buildings, FEMA-273, developed by ATC for FEMA, Washington, D.C., 1997.

[4] Freeman, S.A., The capacity spectrum method as a tool for seismic design. Proc. of the 11th European Conf. on Earthquake Engineering, Paris, 1998.

[5] Ordinanza del PCM n. 3274 del 20/03/2003, Primi elementi in materia di criteri generali per la classificazione sismica del territorio nazionale e di normative tecniche per le costruzioni in zona sismica, 2003.

[6] CEN, Eurocode 8, Design of structures for earthquake resistance, Part 1, European standard prEN 1998-1, Final P Draft, December 2003.
[7] Diotallevi, P.P. & Landi, L., Effect of the axial force and of the vertical ground motion component on the seismic response of R/C frames, Proc. of the 12th World Conf. on Earthquake Engineering, Auckland, 2000.
[8] Scott, B.D., Park, R & Priestley, M.J.N., Stress-strain behaviour of concrete confined by overlapping hoops at low and high strain rates, ACI Journal, pp. 13-27, 1982.
[9] Mwafy, A.M. & Elnashai, A.S., Static pushover versus dynamic collapse analysis of RC buildings, Engineering Structures, 23, pp. 407-424, 2001.
[10] Valles, R., Reinhorn, A. & Kunnath, S., IDARC2D: a computer program for the inelastic analysis of buildings, Technical Report NCEER, 1996.
[11] Diotallevi, P.P. & Landi, L., Valutazione del grado di sicurezza sismica di strutture in c.a. progettate secondo la normative italiana e gli eurocodici, Proc. of the 14th C.T.E. Congress, Mantova, 2002.
[12] Fajfar, P. & Gasperic, P., The N2 method for the seismic damage analysis of RC buildings, Earthquake Engng. Struct. Dyn., 23, pp. 502-521, 1994.
[13] Fajfar, P., Capacity spectrum method based on inelastic demand spectra, Earthquake Engng. Struct. Dyn., 28, pp. 979-993, 1999.
[14] Vidic, T., Fajfar, P. & Fischinger, M., Consistent inelastic design spectra: strength and displacement, Earthquake Engng. Struct. Dyn., 23, pp. 502-521, 1994.